Journal of Alloys and Compounds 509 (2011) 1407–1410

Contents lists available at ScienceDirect

Journal of Alloys and Compounds

journal homepage: www.elsevier.com/locate/jallcom

Two milling time regimes in the evolution of magnetic anisotropy of mechanically alloyed soft magnetic powders

J.J. Ipus[a,b], J.S. Blázquez[a], V. Franco[a], C.F. Conde[a], A. Conde[a,*]

[a] Departamento de Física de la Materia Condensada, ICMSE-CSIC, Universidad de Sevilla, P.O. Box 1065, 41080, Sevilla, Spain
[b] Materials Science and Engineering Departament, Carnegie Mellon University, Pittsburgh, PA 15213, USA

ARTICLE INFO

Article history:
Received 7 September 2010
Received in revised form 25 October 2010
Accepted 28 October 2010
Available online 10 November 2010

Keywords:
Soft magnetic alloys
Amorphous and nanocrystalline alloys
Mechanical alloying and milling

ABSTRACT

The milling time evolution of magnetic anisotropy of ball milled powders can be described considering two regimes. First, for short milling times, the main factor affecting the magnetic behavior of the alloy is the accumulation of internal stresses. Second, for long milling times, magnetic anisotropy can be explained using three contributions: long-range magnetoelastic, averaged short-range magnetoelastic and averaged magnetocrystalline anisotropies.

1. Introduction

Soft magnetic nanocrystalline alloys have been extensively studied since the discovery of Finemet alloys in 1988 [1]. In these alloys, the peculiar two-phase microstructure is responsible for their excellent soft magnetic properties. This microstructure consists of ferromagnetic α-Fe type crystallites (5–20 nm in size) embedded in a residual amorphous phase, also ferromagnetic but with a lower Curie temperature, which enables the magnetic exchange coupling between nanocrystals and averages out the magnetocrystalline anisotropy [2].

Nanocrystalline alloys are metastable systems that require non conventional casting techniques to be produced. Generally, controlled devitrification of a precursor amorphous alloy previously produced by ultrafast quenching techniques (e.g. melt-spinning) is used as the production route. However, nanocrystalline microstructures could be easily obtained by mechanical alloying [3]. Nevertheless, these systems exhibit coercivities some orders of magnitude higher than those of similar alloys obtained by rapid quenching methods [4–6].

The interest in mechanical alloying technique is due to its versatility and suitability to produce nanocrystalline alloys in a much wider compositional range than that achievable by rapid quenching techniques, limited to compositional regions in the vicinity of deep eutectics. Moreover, the subsequent compaction and consolidation of the obtained powder could lead to overcome the shape problem of nanocrystalline alloys obtained by rapid quenching techniques, generally thin ribbons and coatings in order to achieve very high cooling rates.

In recent years, soft magnetism in mechanically alloyed nanocrystalline materials has been studied by Shen et al. [4], concluding that the main contribution to the coercivity in mechanically alloyed powders comes from the long-range fluctuations in the residual stress. In this work this idea has been applied to analyze the coercivity of $Fe_{85}Nb_5B_{10}$ and $Fe_{75}Nb_{10}B_{15}$ compositions prepared by ball milling of elemental powders.

2. Experimental

The two studied compositions were prepared by ball milling in a planetary mill Fritsch Pulverisette 4 Vario from elemental powders (>99% purity) using hardened steel balls and vials. The initial powder mass was 30 g and the ball to powder ratio was 10:1. Two different rotational speeds of the main disk (Ω) were used: 150 and 350 rpm. The power released from the milling media to the powders was found to follow a Ω^3 law [7], which allows us to define an equivalent milling time $t_{eq} = (\Omega/\Omega_0)^3$, being $\Omega_0 = 150$ rpm. The ratio between the rotational speeds of the vials and the main disk was −2. Manipulation of the powders was done under argon atmosphere in a Saffron glove box. Hysteresis loops were recorded at room temperature using a Lakeshore 7407 vibrating sample magnetometer (VSM) with a maximum applied magnetic field $H = 1.5$ T. Saturation magnetization, M_S, was obtained from the extrapolation of high field M(H) curve to zero field.

As powder particles after milling are small (25–250 μm [8]), they can be aligned in an external field by rotation of the whole particle. In order to avoid this effect, which yields an undesirable not good reproducibility of the measurements, powder particles were glued together and encapsulated in an Al foil. Fig. 1 shows the differences between hysteresis loops registered for free powder and glued powder. For free powder, low field susceptibility is higher and coercivity is lower than for glued powder, which is in agreement with the presence of an extra mechanism in

* Corresponding author. Tel.: +34 95 455 28 85; fax: +34 95 461 20 97.
E-mail address: conde@us.es (A. Conde).

0925-8388/$ – see front matter © 2010 Elsevier B.V. All rights reserved.
doi:10.1016/j.jallcom.2010.10.207

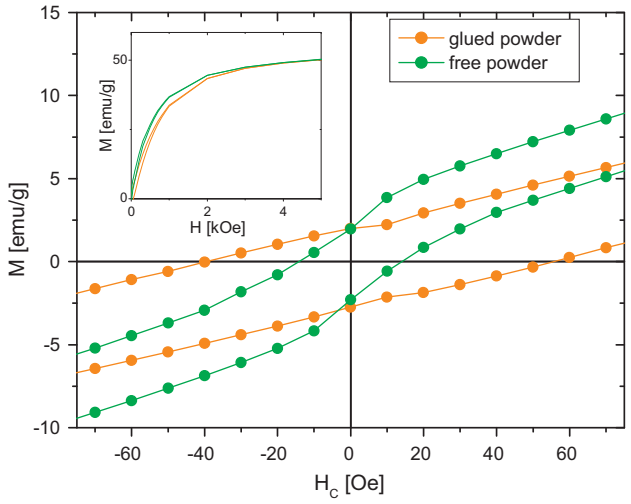

Fig. 1. Low field region of hysteresis loops for free and glued powder samples. The inset shows the first quadrant to appreciate the differences at larger fields.

free powder (rotation of the whole powder particle) to align the magnetic moments with the external field.

3. Results and discussion

Fig. 2 shows the XRD patterns of the studied alloys as a function of the equivalent milling time. A bcc Fe(Nb) supersaturated solution is produced for both alloys but, for the alloy with 10 at.% of Nb, an amorphous phase is also developed at long milling times. Evolution of the microstructure of studied samples with milling time has been detailed elsewhere [8]. Transmission electron microscopy studies have also shown that highly pure boron inclusions remains till the end of the milling time studied [9]. These inclusions are not detected by conventional XRD experiments.

Fig. 3 shows the magnetization and coercivity values obtained from the hysteresis loops for both alloys. Saturation magnetization initially decreases due to the presence of impurities in the neighborhood of Fe atoms, which reduces its magnetic moment, in agreement with the evolution of the hyperfine magnetic field observed by Mössbauer spectrometry [8]. For longer milling times, M_S remains almost constant for the alloy with 5 at.% of Nb, whereas for the alloy with 10 at.% of Nb, it continuously decreases due to the

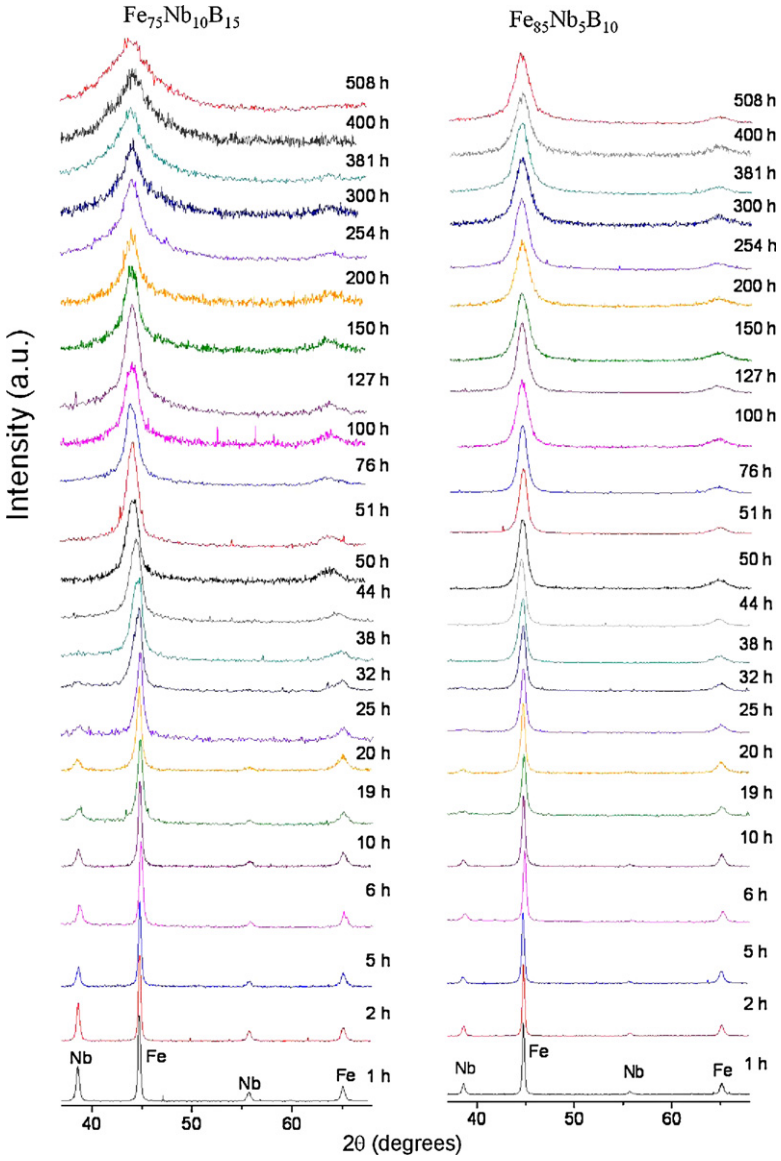

Fig. 2. XRD patterns of the two studied samples as a function of the milling time.

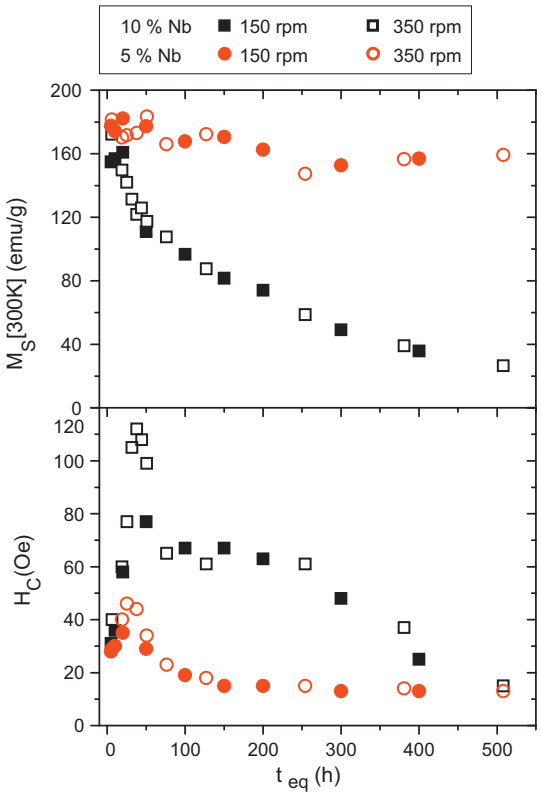

Fig. 3. Room temperature saturation magnetization (above) and coercivity (below) of the two studied alloys as a function of the equivalent milling time.

formation of a paramagnetic amorphous phase (Curie temperature ~250 K [10]).

An initial increase in H_C is observed but, after $t_{eq} \sim 40$ h, coercivity decreases continuously. From H_C and M_S values, an effective anisotropy can be obtained as $K_{eff} = H_C M_S / p_C$ with $p_C = 0.64$ for cubic shape particles [11]. If this parameter is represented as a function of the estimated maximum microstrain of the supersaturated solid solution, obtained from XRD [8], a good linear correlation is obtained for short milling times, as shown in Fig. 4. This linear correlation is lost as milling time increases: microstrain becomes saturated and other effects must be taken into account. As microstrain is proportional to the square root of the dislocation density, a linear dependence of K_{eff} with microstrain is in agreement with

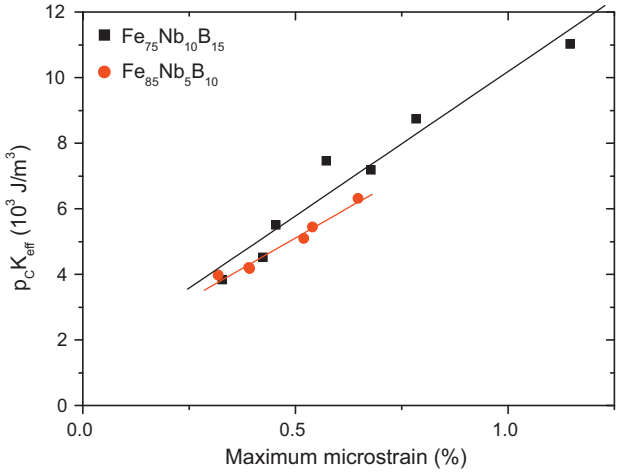

Fig. 4. Effective anisotropy vs. maximum microstrain.

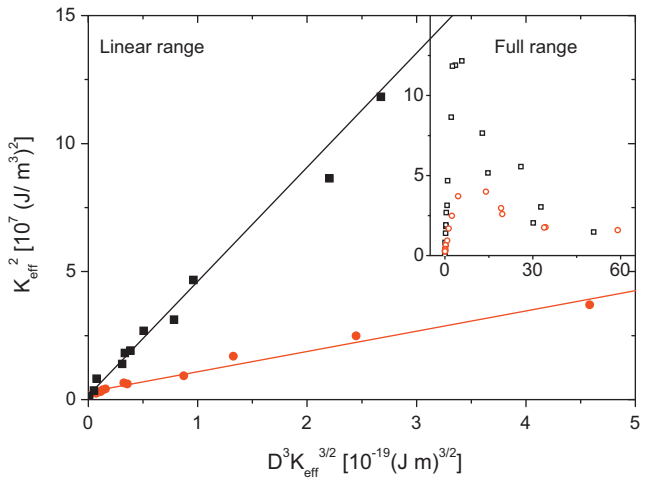

Fig. 5. Linear region of the square of effective anisotropy vs. $D^3K_{eff}^{3/2}$. The inset shows the full range to appreciate the deviation from the linear behavior for short milling times (large crystal size).

previous results [4]. However, the extrapolation to zero microstrain does not lead to zero magnetic anisotropy, unlike found in ref. [4]. This could be ascribed to the presence of boron inclusions in the studied samples, which might contribute to the magnetic hardening of the system.

Following Shen et al. [4], the total anisotropy in a nanocrystalline powder sample, K_{eff}, is the addition of three main contributions: long-range magnetoelastic, $K_{\sigma,ma}$, averaged short-range magnetoelastic, $\langle K_{\sigma,mi} \rangle$, and averaged magnetocrystalline anisotropies, $\langle K_1 \rangle$:

$$K_{eff} = \sqrt{K_{\sigma,ma}^2 + \langle K_{\sigma,mi} \rangle^2 + \langle K_1 \rangle^2} \quad (1)$$

and an implicit equation for K_{eff} can be obtained as:

$$K_{eff} = \sqrt{\left(\frac{3}{2}\lambda_S \sigma_{ma}\right)^2 + \left[\left(\frac{3}{2}\lambda_S \sigma_{mi}\right)^2 + K_1^2\right] \frac{D^3 K_{eff}^{3/2}}{A^{3/2}}} \quad (2)$$

where λ_S is the magnetostriction (−7 ppm for α-Fe [12]); σ_{ma} and σ_{mi} the macro and microstrain, respectively; K_1 is the magnetocrystalline anisotropy ($\sim 2 \times 10^4$ J/m^3 for α-Fe); D is the average crystal size and A the exchange stiffness constant ($\sim 10^{-11}$ J/m).

For long milling times, strains are saturated. Therefore, in this regime, we can plot K_{eff}^2 vs. $D^3 \cdot K_{eff}^{(3/2)}$ as shown in Fig. 5. A good linear correlation is obtained for milling times above 50 h (samples with small crystal size and low coercivity) but the behavior is far from linear for samples milled less time (see the inset in Fig. 5). From the extrapolation to $D = 0$, similar long-range magnetoelastic anisotropies, about 2–3 kJ/m^3 are obtained for both alloys. They are of the same order of magnitude than those found for other Fe based alloys [4]. Taking into account that both magnetostriction and magnetocrystalline anisotropy of the crystalline phase must be similar, the exchange stiffness constant might be obtained from the slope of the regression lines in Fig. 4. Resulting values are ~5 times larger for the alloy with 5 at.% of Nb than for the alloy with 10 at.% of Nb and this could be ascribed to the less efficiency of the paramagnetic amorphous matrix for transmitting the magnetic coupling between ferromagnetic nanocrystals, as predicted by Hernando et al. [2] in their extended theory of magnetic coupling in two phase nanocrystalline systems. Assuming a value of $A = 10^{-11}$ J/m for the alloy with 5 at.% of Nb, and magnetostriction constant, Young modulus and magnetocrystalline anisotropy of bcc Fe, yields $K_{mi} \sim 5 \times 10^4$ J/m^3 and a microstrain of 3%, which is of the order of that obtained from XRD [8].

4. Conclusions

In conclusion, the evolution of the magnetic anisotropy of ball milled powder can be described using two milling time regimes. At low milling times, the progressive increase in the microstrain is responsible for an initial magnetic hardening of the system. After microstrain becomes saturated, the evolution of the magnetic anisotropy is governed by three contributions: long-range magnetoelastic, averaged short-range magnetoelastic and averaged magnetocrystalline anisotropies. The values of the parameters obtained in this study are in agreement with those obtained from other independent techniques.

Acknowledgements

This work was supported by the Ministry of Science and Innovation (MICINN) and EU FEDER (project. No. MAT2010-20537) and the PAI of the Regional Government of Andalucía. J.J.I. acknowledges a Postdoctoral Research Associate position from Carnegie Mellon University.

References

[1] Y. Yoshizawa, S. Oguma, K. Yamaguchi, J. Appl. Phys. 64 (1988) 6044.
[2] A. Hernando, M. Vázquez, T. Kulik, C. Prados, Phys. Rev. B 51 (1995) 3581.
[3] C. Suryanarayana, Prog. Mater. Sci. 46 (2001) 1.
[4] T.D. Shen, R.B. Schwarz, J.D. Thompson, Phys. Rev. B 72 (2005) 014431.
[5] C. Kuhrt, L. Schultz, J. Appl. Phys. 73 (1993) 6588.
[6] P. Crespo, A. Hernando, R. Yavari, O. Drbohlav, A. García-Escorial, J.M. Barandiarán, I. Orúe, Phys. Rev. B 48 (1993) 7134.
[7] J.J. Ipus, J.S. Blázquez, V. Franco, M. Millán, A. Conde, D. Oleszak, T. Kulik, Intermetallics 16 (2008) 470.
[8] J.J. Ipus, J.S. Blázquez, V. Franco, A. Conde, Intermetallics 16 (2008) 1073.
[9] J.J. Ipus, J.S. Blázquez, S. Lozano-Perez, A. Conde, Phil. Mag. 89 (2009) 1415.
[10] J.J. Ipus, J.S. Blázquez, V. Franco, A. Conde, L.F. Kiss, J. Appl. Phys. 105 (2009) 123922.
[11] G. Herzer, IEEE Trans. Magn. 26 (1990) 1397.
[12] R.C. O'Handley, Modern Magnetic Materials Principles and Applications, Wiley, New York, 2000.